Effect of Speed on the Tribological Behavior of Fe–Cu–C Based Self Lubricating Composite

Sanjay Mohan Sharma[1] · Ankush Anand[1]

Abstract In this work, the effect of different speeds on the tribological properties of sintered iron–copper–graphite (Fe–Cu–C) based self lubricating composites have been studied. Fe–Cu–C based self-lubricating composites were prepared by powder metallurgical compaction and sintering method. CaF_2, a solid lubricant in weight percentages of 0, 3, 6, 9 and 12 was added to the base matrix consisting of Fe-2Cu-0.8C. The fabricated samples were tested for friction and wear at a constant load of 10 N and three different speeds of 0.5, 5 and 10 m/s. The surface properties of unworn and worn surfaces were analyzed using optical and scanning electron microscope. The friction and wear test of the composites exhibited decrease in coefficient of friction and increase in wear loss with the increase in speed. The results also revealed different trends in the friction behavior of the developed composites at low (0.5 m/s) and high speeds(5 and 10 m/s). However, at all test speeds, COF of samples with 3, 6 and 9 wt.% was less than the base matrix, and wear loss of 3 wt.% CaF_2 sample was the lowest at all speeds. Ploughing, adhesive and delamination wear were the dominant wear mechanism as revealed by SEM. Based upon the findings, the developed material could be used for low and high speed antifriction applications.

Keywords Fe–Cu–C · Wear · Friction · Speeds · Solid lubricant · CaF_2 · Powder metallurgy

✉ Sanjay Mohan Sharma
   sanjay.mohan@smvdu.ac.in

1   Department of Mechanical Engineering, Shri Mata Vaishno Devi University, Katra, J&K, India

1 Introduction

Self lubricating materials hold an important place in day to day life and, the researchers have been in the process of developing more such materials with high sustainability and low cost. These materials consist of one or more solid lubricants in a base matrix which may be a metal, ceramic, polymer etc. [1–3]. Solid lubricants are the materials which offer lubrication characteristics due to their molecular structure e.g., graphite and molybdenum disulfide (MoS_2) due to their hexagonal structure serve as solid lubricants. The working environment also affects these lubricants such as, in moist conditions graphite is more effective than MoS_2, and in dry conditions it is vice versa. Moreover, various other materials like calcium fluoride (CaF_2), tin, (Sn), antimony (Sb), silver (Ag), tungsten disulfide (WS_2) and boron nitride (BN) have also been tried by the researchers as solid lubricants [4–7]. Apart from this, high oxidation and thermal resistance also plays a vital role in the selection of solid lubricants e.g., magnesium, calcium and barium fluorides exhibit high thermal and oxidation resistance than other lubricants [8–11]. The lubrication ability of fluorides increases with an increase in temperature as it undergoes brittle to ductile transition resulting in low shear strength, thus causing lubrication [12].

Among various metals, iron is being considered as most economical material to be used in metal matrix composites. Iron itself, or with other metals such as copper, graphite, nickel etc., were used as base matrix in various composites [13]. The addition of antimony up to 7.5% in iron resulted in increased hardness and compressive strength [5]. The tribological properties of various steels were improved by solid lubricants such as MoS_2 and hexagonal boron nitride (h-BN) [14–17].

Various fluorides were also tried as solid lubricants in many metal matrices. CaF_2 and BaF_2 were used as solid lubricants in sintered Fe based composites, and CaF_2 was found to exhibit least friction and wear than BaF_2 [18]. The investigation of wear resistance of high-speed steels containing CaF_2, manganese sulfide (MnS) and titanium carbide (TiC) was reported by Childs et al. [19]. The study revealed that the addition of TiC resulted in enhanced wear resistance, whereas self lubricating properties were improved by MnS and CaF_2. Han et al. [20] and Kostornov et al. [21] also reported improvement in the mechanical and tribological properties of sintered iron based materials with CaF_2 as a solid lubricant. The mechanical and tribological properties of Fe–Cu–C based material were improved by adding various metals and solid lubricants to the base matrix as reported by various researchers [15, 16, 22].

The technological advancements demands materials to perform satisfactorily at various operating parameters such as load, temperature, speeds and topography of the contact surfaces. It has been reported by the researchers that these operating parameters strongly influence the friction and wear characteristics of the materials [23–25]. The influence of different speeds on the friction and wear behavior of materials cannot be anticipated, and that's why researchers are investigating tribological properties of materials at different speeds. Plasma nitrided and borided steels were investigated for friction and wear at different speeds with constant load and sliding distance. The study revealed decrease in coefficient of friction and increase in wear resistance of the steels [26]. The increase in speed led to decreased friction values along with increase in wear rate in unlubricated steels [27]. The friction and wear study of AISI 1045 steel coated with Fe–Al showed mixed behavior due to the conditions of different speed and different loads. However, at high load it was observed that coefficient of friction and wear rate decreased with the increase in speed until speed reached to 4 m/s, where both friction and wear rate were higher. The decrease or increase in friction and wear rate at various speeds was attributed to the behaviour of tibo oxide layers [28].

In the present paper, the effect of sliding speed on a newly developed self lubricating composite has been investigated. The composite comprises of Fe–Cu–C as base matrix to which CaF_2 is added in varying percentages. The tests have been conducted at speeds of 0.5, 5 and 10 m/s. All the tests have been carried out at a constant load of 10 N and, the tribological testing has been carried out at room temperature. The surface morphology of unworn and worn samples have been studied using optical and scanning electron microscopy.

2 Experimental Procedure

2.1 Materials and Manufacturing Process

Samples from five different compositions (as shown in Table 1) were fabricated by using uni-axial compaction and sintering process. To ensure homogeneity in the composites, the powders were mixed in a mortar pestle for 15 min, followed by double cone mixing for 30 min. The speed of rotation of the double cone mixer was maintained at 100 rpm. In order to provide lubrication within the powder particles and, between the compact and die walls, zinc stearate was added to the powders. The average particle sizes of iron, copper and, graphite powders were around 75, 50 and 50 μm respectively. The average particle size of CaF_2 powder was about 10 μm. The compaction was carried out in a cylindrical die to obtain green compacts in the shape of cylindrical pins. The compaction was carried out at 600 MPa by means of a hydraulic press. The sintering of the green compacts was carried out at 1120 °C in an inert atmosphere (90% nitrogen and 10% hydrogen) for around 30 min [29, 30]. The purity of iron, copper, graphite and, calcium fluoride powders used in the sample preparation were 99.9, 99.7, 98.5 and, 99% respectively.

2.2 Test Methods and Parameters

The density and hardness of the fabricated samples were investigated. Archimedes principle was used to measure the density of the samples and hardness was measured using Vickers hardness tester. The indentation load for hardness measurement was 50 N and, average value of 5–6 readings for each sample was considered. Friction and wear tests were carried out using a DuCom Wear and friction Monitor TR-20LE-PHM400 pin-on-disc wear test rig. The counterface material used for friction and wear testing was En 31 steel of hardness 60 ± 2HRC and centerline average surface roughness was 1.6 Ra. Friction and wear tests were carried out using cylindrical pins of 8 mm diameter. At the beginning of every friction test, polishing of the samples was carried out with silicon carbide papers of 800 and 1000 grades. Thereafter, the samples were cleaned in acetone and weighed using an electronic weighing balance. Each wear and friction test was carried out at room temperature for a constant load and sliding distance of 10 N and 4000 m respectively. All the tests were conducted at sliding speeds of 0.5 m/s [31], 5 and 10 m/s. In order to ensure the consistency, every test was repeated thrice and, the average values were reported in the text. The friction force was obtained directly from the machine and, the wear loss was determined from the difference in weight of the sample pin measured before and after the test. The surface

Table 1 Chemical composition of the materials (weight %)

Sr. No	Fe	Cu	Graphite	CaF$_2$
1	97.2	2	0.8	0
2	94.2	2	0.8	3
3	91.2	2	0.8	6
4	88.2	2	0.8	9
5	85.2	2	0.8	12

morphology of the as sintered samples was studied by optical microscopy and, scanning electron microscope was used to study the wear mechanisms of the worn out surfaces. The SEM and EDS images were obtained with a JEOL JSM 5600 LV electronic microscope.

3 Results and Discussions

3.1 Density and Hardness

Table 2 shows the density and hardness values of the samples fabricated from various compositions. It is observed that the density of the sintered samples decreases with an increase in the weight percentage of CaF$_2$. Same can be seen from the micrographs as shown in Fig. 1. Amongst all the composites, sample with 3 wt.% CaF$_2$ exhibits highest hardness, which is attributed to the grain refinement of 3 wt.% CaF$_2$ sample as shown in Fig. 1 [20, 32–34]. A continuous decrease in hardness of the samples with 6, 9 and 12 wt.% CaF$_2$ is observed, and this is attributed to decrease in density of the CaF$_2$ added materials.

3.2 Coefficient of Friction (COF)

The friction curves of all the compositions tested at speeds of 0.5, 5 and 10 m/s are as shown in Fig. 2. The presence of oxide layer and contact between less number of asperities initially lead to low values of COF. Thereafter, a sudden rise in the COF is observed which may be due to the formation of a true contact area and removal of oxide

layer leading to metal to metal contact. However, from Fig. 2, it can be seen that a sudden rise in COF is less in samples tested at 10 m/s than those tested at other speeds. This may be due to short running period at a speed of 10 m/s as compared to tests carried out at 0.5 and 5 m/s [35, 36]. The time taken/sliding distance to reach the highest value of COF is more in samples which are subjected to high speed (Fig. 2c) than those at relatively low speed (Fig. 2a, b). However, the COF stabilizes after sliding through a distance of approximately 1000 m. The curves exhibit relatively stable behavior at 0.5 and 5 m/s as compared to 10 m/s. During the investigation, the variation in average COF of all the compositions is between 0.331–0.490. It is also observed that among all tested samples, 3 wt.% CaF$_2$ added sample exhibit the lowest COF at 0.5 m/s speed whereas, at 5 and 10 m/s, COF of 3, 6, and 9 wt.% CaF$_2$ added samples is less than the base matrix.

3.2.1 Effect of Speed on COF

The friction values of the samples have shown a decreasing trend with the increase in sliding speeds (Fig. 3). Similar results have been reported by various authors [37–40]. However, in the present research, decrease in values of COF with rise in speed is attributed to the presence of solid lubricant CaF$_2$. The overall pattern of the COF at low speed (0.5 m/s) is slightly different from that of high speeds (5 and 10 m/s). A gradual decline is observed in COF of the base matrix and 3 wt.% CaF$_2$ samples from 0.5 to 5 m/s. The decline in COF of the base matrix is attributed to thermal softening of the material due to rise in frictional heat at the interface. The decrease in COF of CaF$_2$ added samples is attributed to the weight percentage of solid lubricant (CaF$_2$) and the interfacial temperature, which increases with increase in speed. For instance, a gradual decrease in COF of 3 wt.% CaF$_2$ added sample is due to the presence of low content of CaF$_2$, as compared to sharp decline in the values of COF for 6, 9 and 12 wt.% CaF$_2$ added compositions with an increase in speed from 0.5 to 5 m/s. At high speeds, there is heat generation at the interface which increases the lubrication capability of CaF$_2$, resulting in sharp decline of COF at high percentages

Table 2 Density and Hardness of the materials

Composition (weight %)	Hardness (HV)	Sintered density (gm/cm^3)	Percentage densification
Fe-2Cu-0.8C	90 ± 3	6.30 ± 0.03	80.29
Fe-2Cu-0.8C-3CaF$_2$	128 ± 4	6.11 ± 0.03	79.16
Fe-2Cu-0.8C-6CaF$_2$	84 ± 4	5.87 ± 0.04	77.86
Fe-2Cu-0.8C-9CaF$_2$	78 ± 3	5.61 ± 0.03	75.7
Fe-2Cu-0.8C-12CaF$_2$	67 ± 4	5.41 ± 0.04	74.28
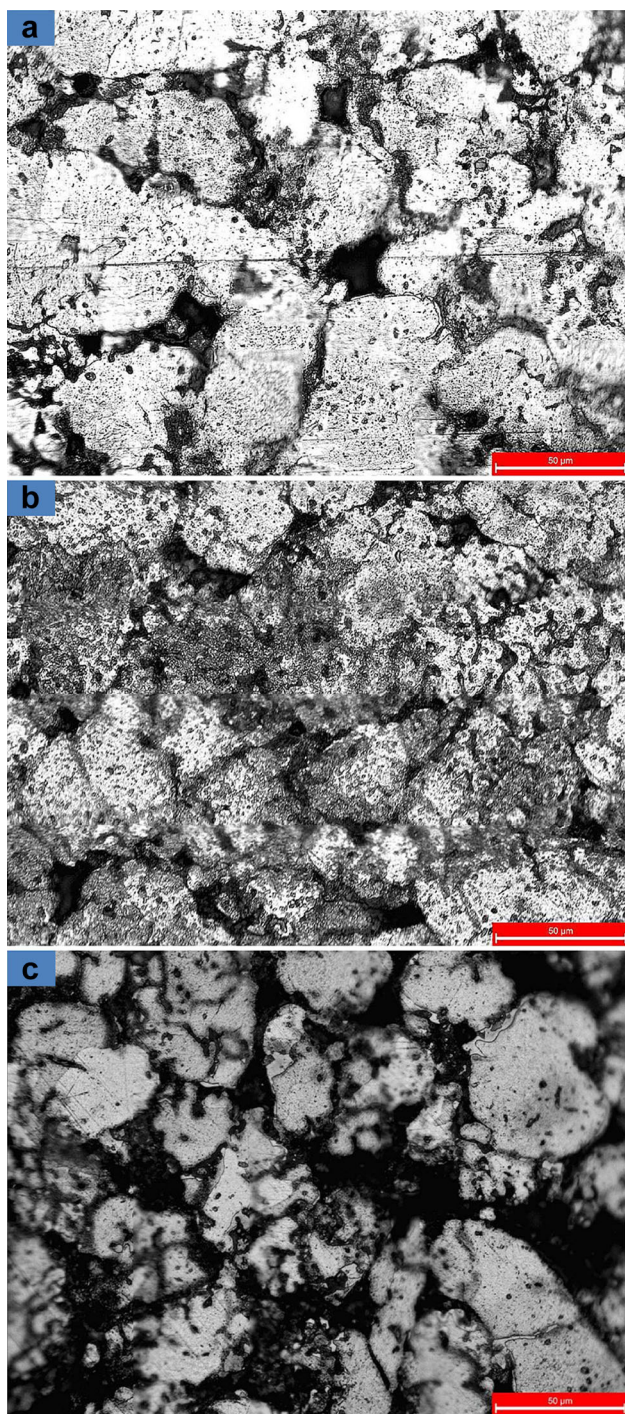
Fig. 1 Optical micrographs of **a** Fe–Cu–C, **b** Fe–Cu–C–3CaF$_2$, **c** Fe–Cu–C–9CaF$_2$

of CaF$_2$. At 5 and 10 m/s, a consistent decrease in COF is observed for all the samples.

Increased speeds result in raised interfacial temperature which in turn results in the formation of tribooxides [28] in addition to the presence of solid lubricant CaF$_2$. The presence of oxides is confirmed from the EDS images as shown in Fig. 4.

3.2.2 Effect of CaF$_2$ on COF

At 0.5 m/s, amongst all the CaF$_2$ added samples, 3 wt.% CaF$_2$ sample exhibits the lowest COF. This is attributed to the lubrication behavior of CaF$_2$, which increases with the increase in temperature [10]. However, at 0.5 m/s, heat generation at the interface is quite less as compared to other speeds, and this amounts to partial adhesion. Due to this partial adhesion, CaF$_2$ causes adhesion which in turn increases friction with the increase in CaF$_2$ contents. This is the reason for increased COF at 6 wt.% CaF$_2$ and onwards at 0.5 m/s. At increased speeds, friction values of CaF$_2$ added samples are less than base matrix, except for 12 wt.%. A decreasing trend is observed in friction up to 6wt.% CaF$_2$, followed by an increasing trend from 9 to 12 wt.% CaF$_2$. The decreasing trend is due to the decrease in the shear strength of CaF$_2$ at increased temperature which enhances the lubrication capability of CaF$_2$ [10, 12]. However, the increasing trend in COF is attributed to the dominance of hard iron oxides over solid lubricant. Due to increased interfacial temperature, more oxides are formed in samples with increased porosity as in 9 and 12 wt.% CaF$_2$ samples. These tribo oxides formed dominates the lubrication capability of CaF$_2$, thus raising the friction values. EDS images as shown in Fig. 4 confirm the presence of oxides in base matrix and CaF$_2$ added samples.
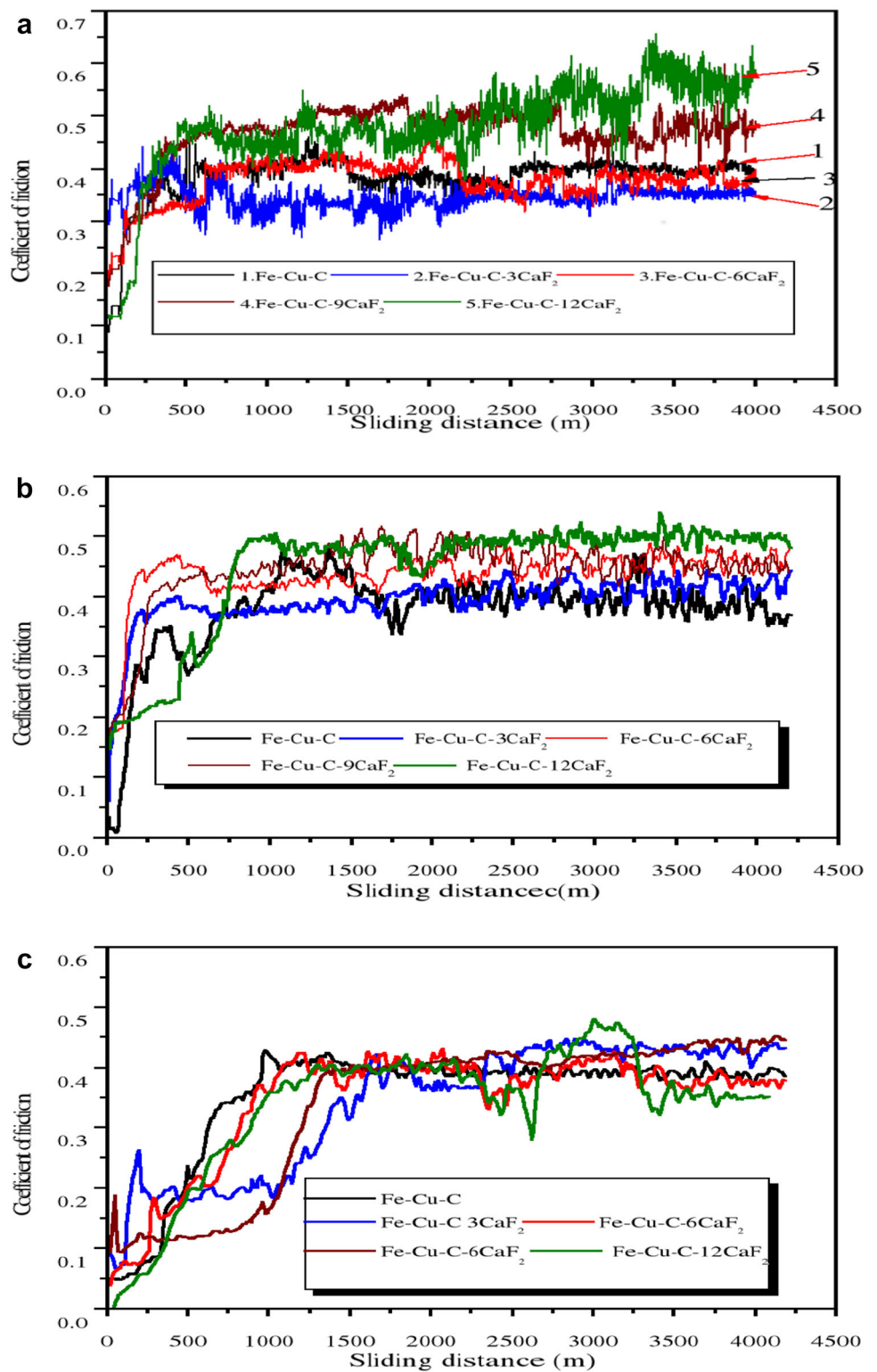
3.3 Wear Loss

The wear loss of the material at different speeds is determined by the difference in weight of the sintered steel pin measured before and after the test.

3.3.1 Effect of Speed on Wear Loss

The average wear loss of samples investigated at 0.5, 5 and 10 m/s is as shown in Fig. 5. It is observed that the wear loss increases with the increase in speed. This may be attributed to the decreased strength of the material due to frictional heat generated at the contact surface. At high speeds, the frictional heat softens the material at the interface, and thus results in reduced shear strength of the material. The softening of materials at high speeds leads to enhancement of true contact area which results in increased adhesive and abrasive wear loss (Fig. 6). Increased adhesion is one of the factors in decreasing friction but results in increased wear loss. The increase in wear loss is also attributed to the unstable behaviour of oxides. The weak bonding between the oxides and the substrate results in high rate of oxide removal than its formation [31, 41]. The hardness may have decreased with the rise in interfacial temperatures due to high speeds, resulting in the increased wear loss with the rise in speeds [26, 42].

Fig. 2 Friction Curves of all compositions at **a** 0.5 m/s [31], **b** 5 m/s, **c** 10 m/s


3.3.2 Effect of CaF₂ on Wear Loss

The wear loss in base matrix is due to the thermal softening of the material, leading to increased adhesive wear. Amongst all the samples, wear loss of 3wt.% CaF$_2$ added sample is observed to be the lowest at all test speeds. This is attributed to hardness and weight percentage of CaF$_2$. Due to high hardness of 3 wt.% CaF$_2$ sample, the counterface material asperities penetrate less as compared to other compositions. Secondly, lowest wear loss is

Fig. 3 Average COF of all compositions
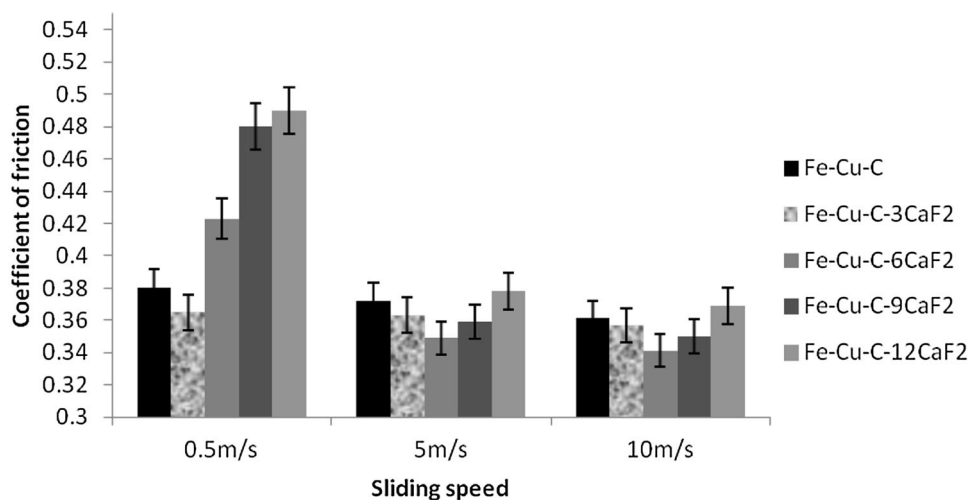
Fig. 4 EDS images of worn out surfaces of **a** Fe–Cu–C and **b** Fe–Cu–C–3CaF$_2$
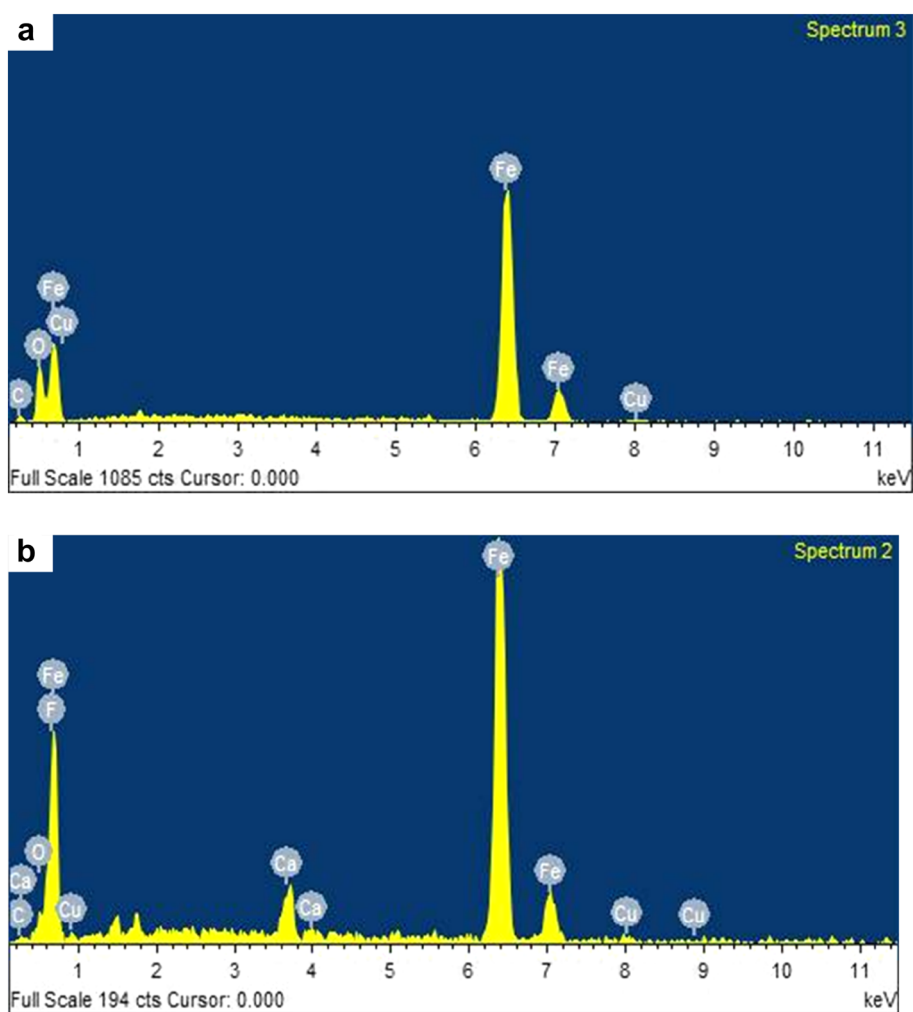
attributed to the partial adhesion of CaF$_2$. Due to decrease in the shear strength at high temperatures, CaF$_2$ undergoes brittle to ductile transition and thus causes lubrication [10]. However, the present tests being carried at room temperature does not generate sufficient high temperatures at the interface, which results in partial adhesion with increase in wt.% of CaF$_2$, causing increased adhesive wear.

Fig. 5 Wear loss of all compositions
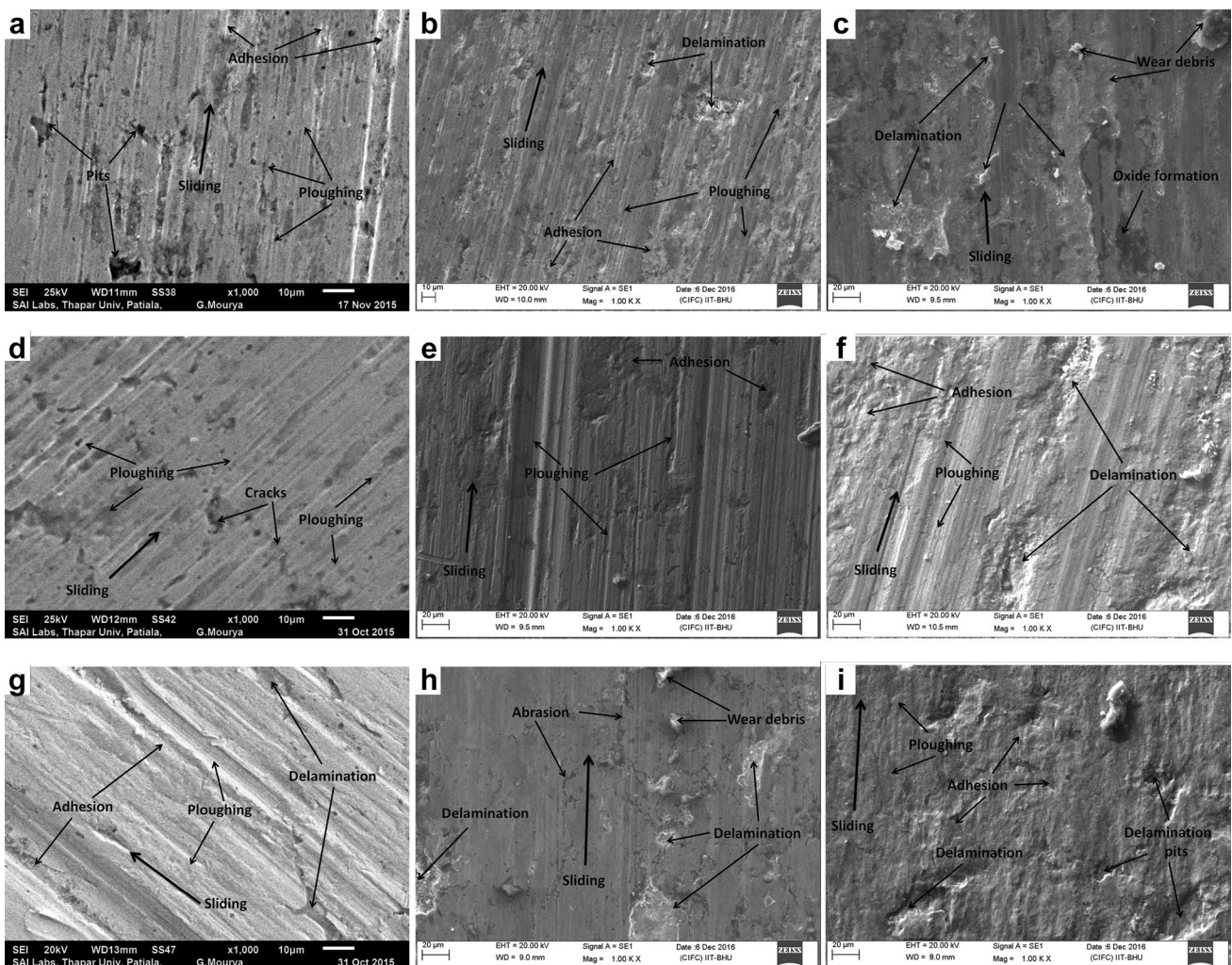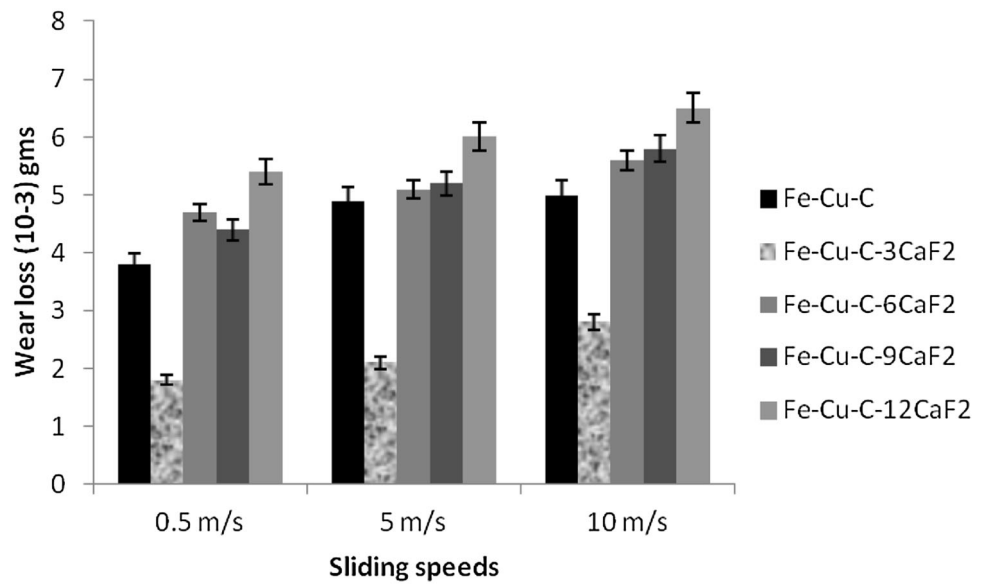
Fig. 6 SEM images of worn surfaces of Fe–Cu–C at, **a** 0.5 m/s, **b** 5 m/s, **c** 10 m/s; Fe–Cu–C-3CaF$_2$ at, **d** 0.5 m/s, **e** 5 m/s, **f** 10 m/s; Fe–Cu–C–9CaF$_2$ at, **g** 0.5 m/s, **h** 5 m/s, **i** 10 m/s

Increase in wear loss in compositions except 3 wt.% CaF_2 may be attributed to the hardness of the composites (Table 2), which decreases with the increase in CaF_2 percentage. Increased adhesion is also attributed as one amongst other reasons for increased wear. As discussed above, at room temperature, sliding doesn't generate high temperatures, which aid CaF_2 to adhere properly to the substrate and result in improved tribo properties. Due to this very reason, partial adhesion take place which lead to adhesive wear and delamination. Increased weight percentage of CaF_2 results in increased delamination and same can be observed from the SEM images as shown in Fig. 6.

3.4 Worn Surface Analysis

In this study, wear of the materials is attributed to distinct wear mechanisms. Figure 6a shows that at 0.5 m/s, adhesion along with ploughing has occurred in the base matrix, but the former seems to be more prominent than the later. Cracks and cavities are also observed in the base composition. The cavities formed are aligned in the direction parallel to the sliding and the cracks are inclined at a certain angle to the direction of sliding. The increase in adhesion and ploughing in the base matrix at 5 m/s is observed in Fig. 6b. Delamination is also seen in Fig. 6b, indicating increased wear rate with the increase in speed. Figure 6c shows more increase in wear due to increased delamination and adhesion at 10 m/s. Some worn out particles from the material also lead to third body abrasion causing an increase in wear. At 0.5 m/s, 3 wt.% CaF_2 added sample is subjected to less ploughing and adhesion as compared to the base matrix (Fig. 6d). The cracks generated can also be seen in Fig. 6e. It is observed that most of the cracks are formed in the direction perpendicular to the direction of sliding. At high speeds, an increase in ploughing is observed with adhesion at certain locations (Fig. 6f). Adhesion may be due to raised temperature at the interface causing CaF_2 to adhere to the surface, thus reducing friction. Adhesion becomes more prominent at 10 m/s and delamination regions can also be spotted, which indicate increase in wear loss. It is observed from Fig. 6g that at 0.5 m/s, the effect of ploughing in 9 wt.% CaF_2 added sample is more as compared with 0, and 3 wt.% CaF_2 added samples. Ploughing and delaminated regions can also be seen in Fig. 6h, i. There is increase in adhesion and delamination wear at high speeds which indicate increase in wear.

From the SEM images, it can be concluded that with the increase in speed, wear mechanisms at low speed have intensified at high speeds. Delamination, mostly is seen at high speeds and also in samples with less density (high porosity), depicting increase in wear. Increased adhesion in the samples also adds to increase in wear but have reduced

friction. It is observed from the above mentioned SEM images that worn surfaces of 3wt.% CaF_2 added sample are relatively smoother than rest of the samples, which indicates better friction and wear properties.

4 Conclusions

A self lubricating composite comprising of Fe–Cu–C as base matrix and, CaF_2 as a solid lubricant additive was developed during the study. Tribological testing was carried out for the developed materials at different speeds and, following conclusions could be drawn from the results:

1. The density of Fe–Cu–C–CaF_2 decreased with an increase in the weight percentage of CaF_2. The composite with 3 wt.% CaF_2 exhibited highest hardness due to grain refinement and beyond 3 wt.% CaF_2, hardness followed a decreasing pattern due to a decrease in density.
2. The speeds ranging from low to high influenced the friction and wear behaviour of the developed composites i.e., friction of all the composites decreased with the increase in speed, where as wear loss increased.
3. A decreasing pattern was observed in the friction values from base matrix to 6 wt.% CaF_2, followed by an increasing pattern up to 12 wt.% CaF_2. Despite the different patterns, friction values of CaF_2 added samples up to 9 wt.% were less than that of base matrix.
4. Fe–Cu–C–3CaF_2 composition showed the lowest wear loss due to its highest hardness at all the test speeds.
5. The SEM microscopy revealed that wear mechanisms such as, adhesion, ploughing and delamination were prominent along with crack formation at certain places.

References

1. Ding CH, Liu CH, Yang ZM, Wang YP, Sun ZB and Yu L, *Compos. Sci. Tech* **70** (2010) 1000.
2. Kato H, Takama M, Iwai Y, Washida K and Sasaki Y, *Wear* **255**(2003) 573.
3. Dhanasekaran S, and Gnanamoorthy R, *Mater Des* **28** (2007)1135.
4. Sliney HE, *Tribol Int* **15** (1982) 303.

5. Verghese R and Gopinath K, *Key Eng. Mater* **29** (1988) 457.
6. Lansdown A R, Wiley, New York (1994).
7. Sliney H E *ASLE Trans*, **29** (1986) 370.
8. Shevchuk Y F, *Powder Metall Met Ceram* **40** (2001) 40.
9. Miroshnikov V N, and Shevchuk Y F, *Powder Metall Met Ceram* **10** (1971) 911.
10. Fedorchenko I M, Zozulya V D, and Shevchuk Y F, *Powder Metall. Met. Ceram* **9** (1970), 818
11. Singh N, Mir I U, Raina A, Anand A, Kumar V and Sharma S M *J. Alex. Eng* (2017) May 27.
12. Wang H M, Yu Y L, and Li S Q, *Scr Mater* **47** (2002) 57.
13. Sharma SM and Anand A, *Tribol. Ind* **38** (2016) 318
14. Dhanasekaran S and Gnanamoorthy R *Mater Sci Eng* (2004).
15. Dhanasekaran S, and Gnanamoorthy R, *J Mater Sci* **42** (2007) 4659.
16. S. Dhanasekaran and R. Gnanamoorthy, *Mater. Des.*, **28** (2007) 1135.
17. Mahathanabodee S, Palathai T, Raadnui S, Tongsri R and Sombatsompop N, *Adv Mat Res*, **747** (2013), 307.
18. Shevchuk Y F, Zozulya V D and Khrienko A F, *Powder Metall. Met. Ceram* **7**(1968), 985.
19. Zuomin L, and Childs T H, *Wear* **257** (2004) 435.
20. Han J, Jia J, Lu J, and Wang J, *Tribol. Lett* 34 (2009) 193.
21. Kostornov A G, Fushchich O I, Gorban V F, Chevychelova T M, and Kostenko O D, *Powder Metall Met Ceram* **51** (2012) 412.
22. Merie V V, Cândea V C, Bîrleanu C, Păşcuţă P, and Popa C O, *J Compos Mater* **48** (2014).
23. Kim DW and Kim KW, *Wear* **315**(2014) 95-102.
24. Li H, Yin Z, Jiang D, Jin L and Cui Y, *Wear* **328** (2015) 17.
25. Thakare M R, Mason J F, Owen A K, Gillespie D R, Wilkinson A J and Franceschini G, *Tribol. Int* **96** (2016) 373.
26. Gunes I, *Mater. Tehnol*. **49** (2015) 111.
27. Earles S W and Kadhim M J, *Proc. Inst. Mech. Eng.* **180** (1965) 531.
28. Zhou Y, Wang SQ, Zhang BG, Zhang QY and Zhou DQ, *Tribol. Trans* (2017) 1
29. Nekatibeb F, Annamalai A R and Upadhyaya A, *Trans Ind Inst Met* **64** (2011) 81
30. Upadhyaya A, Upadhyaya GS, *Powder Metallurgy Science, Technology and Materials.* Universities Press (2011)
31. Sharma S M, Anand A, *Ind. Lub Tribol* **69** (2017) 715.
32. Zhang A M, Hai H A, and Zhang X G, *Trans Non Ferr Met Soc China* **23** (2013) 3167.
33. Oh J M, Lim J W, Lee B G, Suh CY, Cho SW, Lee S W, and Choi G S, *Mater Trans* **51** (2010) 2009.
34. Song KH, Kim HS and Kim WY, *Rev Adv Mater Sci*. **28**(2011) 158.
35. Paleu V, *Mech. Test. Diag*. (2012), 27.
36. Guezmil M, Bensalah W, Khalladi A, Elleuch K, De-Petris Wery M and Ayedi H F, *Inter. Sch. Res. Not.* (2014).
37. Gopinath K, Rayudu G V, Narayanamurthi R G, *Wear* **42**(1977) 245.
38. So H, Yu DS and Chuang CY, *Wear* **253** (2002) 1004-15.
39. Rajkumar K and Aravindan S, *App. Mech. Mater* **592** (2014) 1305.
40. Molinari A, Straffelini G, Tesi B, Bacci T and Pradelli G, *Wear* **203** (1997) 447.
41. Straffelini G and Molinari A, *Tribol. Lett* **41** (2011) 227-238.
42. Nakahara T, Momozono S and O-rui A, *J. Eng. Tribol.* **224** (2010) 271.